Materials Research Society Symposium
Proceedings Vol. 838E, 2005, 014.11.1 – 014.11.6

TEM investigation of nucleation and initial growth of ZnSe nanowires

Y. Cai, S.K. Chan, I.K. Sou, Y.F. Chan, D. S. Su[1] and N. Wang

Physics Department and the Institute of Nano Science and Technology, the Hong Kong University of Science and Technology, Hong Kong, China
[1] Department of Inorganic Chemistry, Fritz Haber Institute of the Max Planck Society, Faradayweg 4-6, D-14195 Berlin, Germany

ABSTRACT

Single crystalline ZnSe nanowires were fabricated on GaAs substrates by molecular beam epitaxy technique via Au-catalyzed vapor-liquid-solid reaction. The nucleation and initial growth of the nanowires were investigated by high-resolution transmission electron microscopy. It was revealed that Au catalysts initially reacted with the substrate forming binary $AuGa_2$ alloy droplets. The sizes of the catalysts determined the growth direction of ZnSe nanowires. A model based on the surface energies of the nanowire nuclei was proposed to explain the size dependence of growth direction for ZnSe nanowires.

INTRODUCTION

The vapor-liquid-solid (VLS) [1] technique has been widely used for growing onedimensional (1D) semiconductor nanostructures because the nucleation sites and the diameters of the 1D nanostructures can be well-controlled by the pre-formed metal catalysts. In recent years, ultrathin semiconductor nanowires [2-4] synthesized based on the VLS and other chemical vapor deposition techniques have shown interesting properties, and some 1D nanostructures have potential use in a variety of technological applications [5-7]. To better control the morphology, atomic structure and defect density of as-grown 1D semiconductor nanostructures or to make these nanostructures with well-organized arrangement, metal-catalyzed chemical-beam epitaxy (CBE) [8] and molecular-beam epitaxy (MBE) [9] techniques have been employed to grow both III-V and II-VI compound semiconductor nanowires.

In our previous work [10], we reported MBE growth of ZnSe nanowires on GaP(111) substrates. The growth process was based on the Au-catalyzed VLS. We have observed that ultrathin ZnSe nanowires contain few defects, and show interesting growth phenomena. ZnSe nanowires may grow along <111>, <112> or <110> directions on the same substrate. For ZnSebased and II-VI semiconductor devices, high density defects, such as dislocations and stacking faults formed in the early growth stage at the substrate interface, are the main reason causing device degradation. 1D ZnSe nanostructures we synthesized generally contain few defects and hence are expected to provide exciting possibilities for technical application. The catalytic growth process of compound semiconductor nanowires is much complicated compared with that of Si or Ge. It is generally believed that ternary alloy catalysts should form to catalyze the growth of compound semiconductor nanowires. In this paper, we report the nucleation and initial growth of Au-catalyzed ZnSe nanowires on GaAs substrates. Binary Au-Ga alloy catalysts have been found to play an important role in influencing the growth direction of ZnSe nanowires.

Materials Research Society Symposium
Proceedings Vol. 838E, 2005, 014.11.1 – 014.11.6

EXPERIMENTAL DETAILS

ZnSe nanowires were grown on GaAs (111), (110) and (001) substrates in a VG V80H MBE system dedicated to ZnSe-based II-VI compound growth in a single chamber. Details of the experimental condition can be found in our previous publication [10]. A thin Au layer (0.3 0.6nm thick) was deposited on the substrate at 150°C. Au nanoparticles formed on the substrate surface by an annealing process at 530°C for 10 minutes. Then, ZnSe nanowires were grown at 530°C using a ZnSe compound-source effusion cell. The nucleation process of Au catalyst particles and the initial growth of ZnSe nanowires on different substrates were investigated by high-resolution transmission electron microscopy (HRTEM). The chemical composition of the catalysts and nanowires were characterized by electron energy-loss spectroscopy (EELS) in a JEOL 2010F field-emission gun transmission electron microscope (TEM) equipped with a Gatan ENFINA EELS system.

DISCUSSION

To eliminate the artifacts introduced from specimen preparation, the as-grown ZnSe nanowire samples were directly observed by the reflection electron microscopy (REM) mode in the TEM. Similar to our previous observation, ZnSe nanowires with diameters smaller than 20nm grew only along <110> direction. Fig.1 (a) and (b) illustrate the typical morphology of ZnSe nanowires grown on GaAs (001) and (110) substrates respectively. All ZnSe nanowires have spherical catalyst tips, indicating the typical VLS growth process. Fig.1 (a) was taken with the electron beam nearly parallel to the [100] direction of GaAs(001) substrate. Long grew mainly along two directions inclined approximately ±45° to the normal of the substrate surface. When observed along the [010] direction, the nanowires showed similar inclinations. Obviously, these nanowires grew along the four <110> directions of the substrate. ZnSe nanowires grown on GaAs(110) substrate are generally perpendicular to the substrate surface, i.e., along the [110] direction. This growth direction was also confirmed by electron and high-resolution TEM images (see Fig.2 (a)) taken from individual ZnSe nanowires. In addition, thin ZnSe nanowires (diameter < 20nm) grown by the present technique contain few defects.
To study the structure change of Au catalysts during the initial growth stage, Au was deposited on the GaAs (111) surface and then annealed at 530oC to form uniform Au droplets

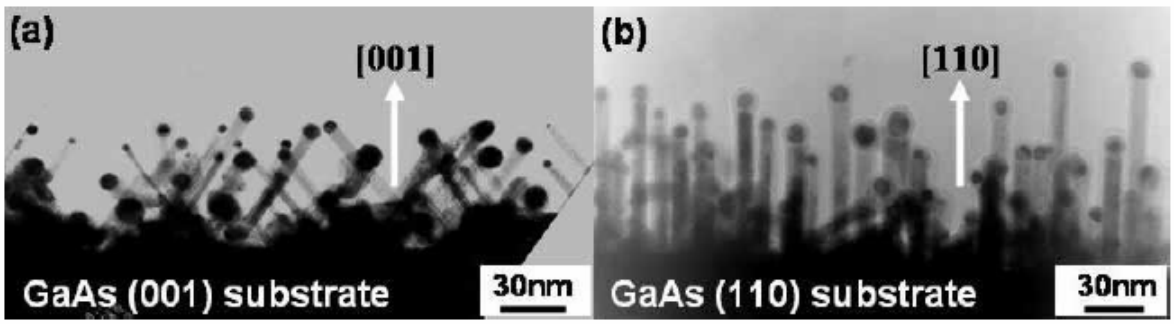

Figure 1 REM images showing ZnSe nanowires grown on (a) GaAs (001) and (b) (110) substrate surfaces.

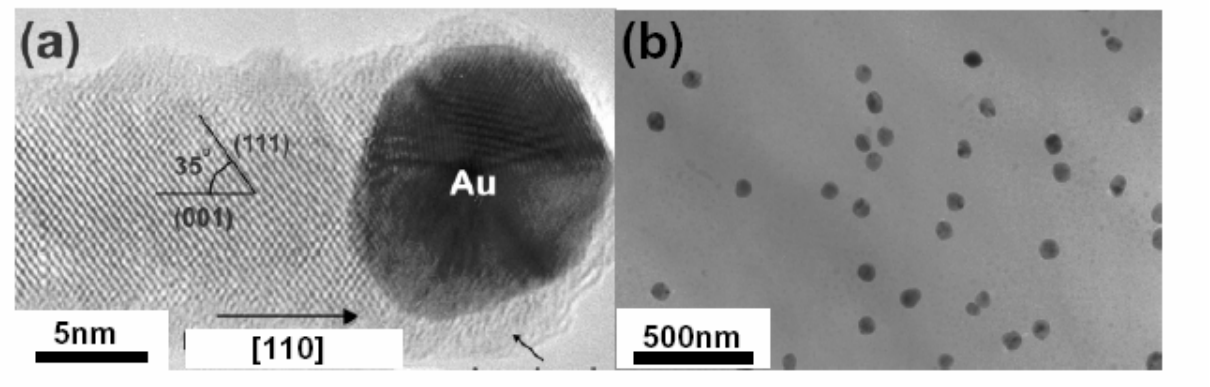

Figure 2 (a) HRTEM image of a ZnSe nanowire grown along [110]. (b) Plan-view of Au catalysts formed on the substrate surface by the annealing treatment.

without depositing ZnSe. Fig. 2 (b) is a plan-view TEM image of Au particles formed by the annealing treatment. The size and density of the particles were controlled by the thickness of predeposited Au layer and the annealing time. Fig. 3(a) is an enlarged image showing the morphology of Au catalysts in which 2D moiré patterns are clearly visible. However, the spacings of the moiré fringes were not due to the overlap between GaAs substrate and FCC Au structure. The selected-area electron diffraction (SAED) pattern from this particle (Fig.3 (b)) illustrates clearly GaAs [111] zone diffractions surrounded by satellite spots. Through systematical observation in different orientations and image simulation, we identified that all catalysts were $AuGa_2$ FCC structure (space group Fm3m, lattice parameter a = 0.6073nm). As shown in the SAED pattern in Fig.3 (b) (along [111] zone axis) and Fig.3 (c) (along [112] zone axis), $AuGa_2$ forms epitaxially on the substrate with orientation relationship of $[100]_{GaAs}//[100]_{AuGa_2}$ and $[010]_{GaAs}//[010]_{AuGa_2}$. Fig. 3(d) shows the cross-sectional view of an $AuGa_2$ catalyst. We observed that all catalysts have reacted with the substrate after the annealing treatment. The sharp interface between the catalyst and the substrate has moved toward the substrate compared to neighboring substrate surface. The chemical composition of the catalysts has been characterized using EELS and x-ray energy dispersive spectroscopy (EDS), and the results indicated that the catalysts consisted of Au and Ga. However, no As was detected in the catalysts. The interface between the catalyst and substrate (about 7.4% mismatch) is (111) at which interfacial dislocations have been observed. It is unknown why $AuGa_2$ binary alloy (not Ga-As-Au ternary alloy) was resulted by the reaction between Au and GaAs substrate, and why As did not participate the ZnSe nanowire growth. The reaction of the catalysts could be described as

$$2\,GaAs + Au \longrightarrow AuGa2 + 2As\uparrow \qquad (1.)$$

In this reaction, As could be extracted from the substrate during the formation of $AuGa_2$ alloy. Then, As might diffuse out of the catalyst surface to be evaporated. A similar reaction was observed when Au catalysts formed on a ZnSe buffer surface. Au reacted with ZnSe forming ZnAu alloy droplets and Se was evaporated out of the droplets. We have characterized the impurities in ZnSe nanowires catalyzed by $AuGa_2$. No Se, Ga or Au was detected by EDS and EELS.

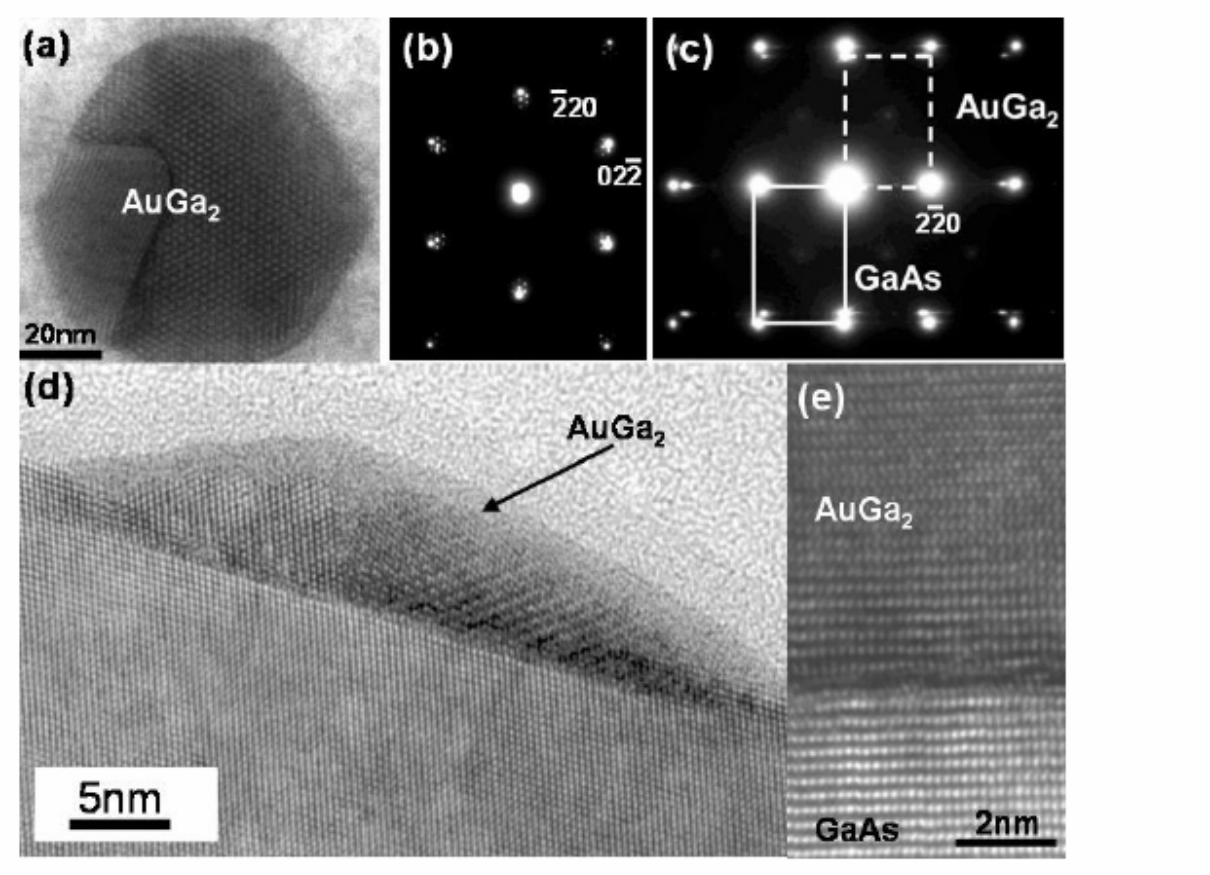

Figure 3 (a) Plan-view of the catalyst. (b) and (c) SAED patterns taken along the [111] and [112] zone axes of the catalyst respectively. (d) HRTEM cross-sectional view (along [110] direction) of the catalyst formed on the substrate. (e) The catalyst interface structure viewed along [112] direction.

It is interesting to note that all ZnSe nanowires with diameters greater than 30nm prefer growing along <111> direction on GaAs (111) or (001) substrates. Those ZnSe nanowires have diameters of 20 - 30nm generally grow along [112] direction on these substrates. While thin ZnSe nanowires (diameters < 20nm) always show [110] growth. We believe that the catalysts and initial growth stage play an important role for the growth direction of ZnSe nanowires. Here, we propose a model based on our observation of the nanowire structure and the principle that crystalline nucleation favors the minimum of the total system energy to understand the above size dependence of nanowire growth direction.
We consider the nucleus of a nanowire as a column with two interface planes and a cylindrical side surface. Because the surface to volume ratio is high and the bulk crystal energy is independent of orientation, surface energies determine the total system energy. For nanosized crystals, a cylindrical side surface actually consists of low energy surfaces and steps. As shown in Fig.3 (a), a hexagonal shape is a good approximation to describe the cross section of a nanocatalyst or a nanowire [11]. Thus, the total energy of a nanowire is:

$$F = \sum A\gamma_s + E_e \qquad (2.)$$

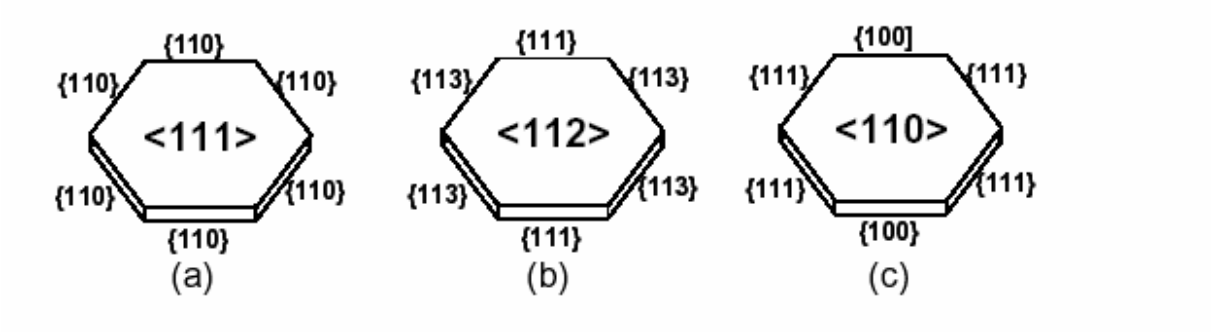

Figure 4 Model of the nanowire nuclei grown along (a) <111>, (b) <112> and (c) <110> directions in a hexagonal geometry with two interfaces and six side faces.

Here, γ_s and E_e represent the surface energy and edge/step energies respectively. A is the area of the surface. For the hexagonal shape approximation, E_e can be considered as a fixed term for different oriented nanowires with a hexagonal shape. Thus, only surface energies need to be considered for the nanowire nuclei. As schematically shown in Fig. 4, the initially formed nanowires should like hexagonal disks. The top and bottom surfaces are interfaces with the catalyst and the substrate, respectively. For the three growth directions observed in our samples, the most possible side surfaces are shown in this figure. The side surfaces can be {111}, {110}, {113} and {100}. Based on the previous work of Eaglesham *et al*.[12], the relationship betweenthe surface energies of these surfaces for a Si crystal is $\gamma_{\{111\}} < \gamma_{\{100\}} < \gamma_{\{112\}} \approx \gamma_{\{113\}} < \gamma_{\{110\}}$. Since ZnSe (zinc blende) and Si (diamond) have similar cubic structure, it is very likely that this relation can also be applied to ZnSe nanowires. For <111> oriented nanowires, the top and bottom surfaces are {111} (the lowest energy surface) and the six rectangular side surfaces should be all {110} surfaces in order to minimize the total surface energy. The nanowires grown along <111>, <112> and <110> should have a total system energy in an increasing order. This is because in the initial nucleation, the side surface area is relatively insignificant. Nanowires will prefer to grow along the <111> direction due to the fact that {111} interface has the lowest surface energy. When the length of a nanowire nucleus exceeds certain value, <111> growth may not offer the minimum state for total surface energies. This can be seen in Fig.4(c) in which the <110> (highest energy surface) growth results in four {111} and two {100} side surfaces (all have low surface energies). We believe that there is a terminal growth zone in the order of a few monolayers where the atoms are nearly in a molten state during growth. Within this zone, the change of growth orientation of a nanowire can be triggered to favor lower total system energy. If the size of the catalyst is large, the contribution of the two interfaces in the total system energy will be always dominant within the terminal growth zone so that it will keep on growing along the <111> direction. For nanowires grown under small size catalysts, within the thickness of the terminal growth zone, the contribution from the side surface will be largely increased. As a consequence, this triggers a transition in growth direction to reach a lower total system energy that is either along <110> or <112>. For ultrathin nanowires, <110> growth will be more energetically favorable. The prediction from this model is in fact in good agreement with our observations.

We have observed growth direction transition of ZnSe nanowires as illustrated in Fig.5. The diameter of the nanowire root is about 33nm. This nanowire shows <111> growth feature on its lift side, but <112> growth on its right side. The diameter near the top of this short nanowire is

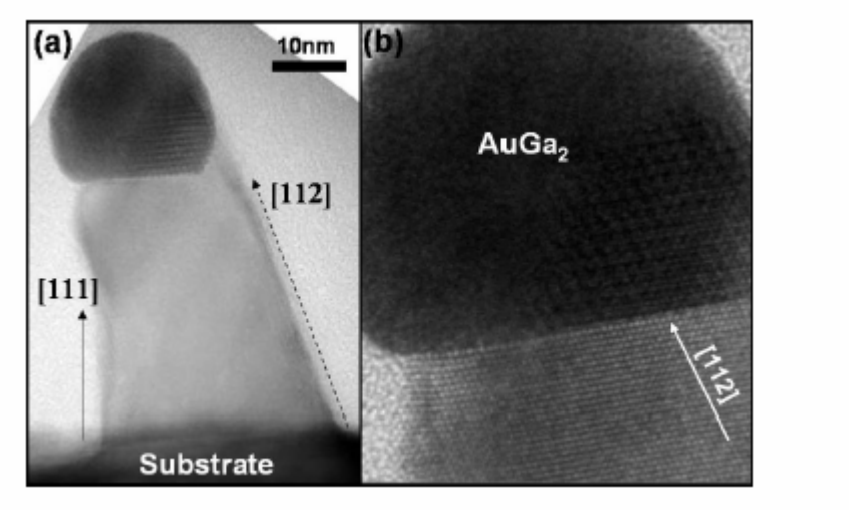

Figure 5 (a) Initial growth of a ZnSe nanowire. The growth direction changed from [111] to [112] due to the change of the nanowire diameter. (b) Enlarged image showing the catalyst interface structure.

reduced from 33nm to 22 nm. The growth direction is then totally changed to <112> at the top of the nanowire. The lattice orientation in semiconductor nanowires is important because it may affect their optical and transport properties. The present work also provides an effective way of fabricating and controlling the morphology of as-grown II-VI semiconductor nanostructures or to make nanostructures with controlled crystalline orientation.

ACKNOWLEDGMENTS

This work was supported by Research Grant Council of Hong Kong (project No. 603804, DAG03/04.SC27 and G_HK019/03).

REFERENCES

1. R. S. Wagner and W. C. Ellis, *Appl. Phys. Lett*. **4,** 89 (1964).
2. A. M. Morales and C. M. Lieber, *Science,* **279,** 208 (1998).
3. N. Wang, Y.F. Zhang, Y.H. Tang, C.S. Lee, and S.T. Lee, *Appl. Phys. Lett*., **73,** 3902 (1998).
4. D. P. Yu, Z. G. Bai, Y. Ding, Q. L. Hang, H. Z. Zhang, J. J. Wang, Y. H. Zou, W. Qian, G. C. Xiong, H. T. Zhou, and S. Q. Feng, *Appl. Phys. Lett.* **72**, 3458 (1998).
5. D. Appell, *Nature (*London) **419**, 553 (2002).
6. J. D. Holmes, K.P. Johnston, R. C. Doty, and B. S. Korgel, *Science* **287**, 1471 (2000).
7. M. S. Gudiksen, L. J. Lauhon, J. Wang, D. C. Smith, and C. M. Lieber, *Nature* (London) 415, 617 (2002).
8. M. T. Björk, B. J. Ohlsson, T. Sass, A. I. Persson, C. Thelander, M. H. Magnusson, K. Deppert, L. R. Wallenberg, and L. Samuelson, *Appl. Phys. Lett.* **80**, 1058 (2002).
9. Z. H. Wu, X. Y. Mei, D. Kim, M. Blumin, and H. E. Ruda, *Appl. Phys. Lett.* **81**, 5177 (2002)
10. Y. F. Chan, X. F. Duan, S. K. Chan, I. K. Sou, X. X. Zhang, N. Wang, *Appl. Phys. Lett*. **83**, 2665 (2003).
11. Y. Zhao and B. I. Yakobson, *Phys. Rev. Lett*. **91**, 35501(2003).
12. D. J. Eaglesham, A. E. White, L. C. Feldman, N. Moriya, and D. C. Jacobson, *Phys. Rev. Lett*.**70**, 1643(1993).